3.2.2 The phylogeny of *Maladera* (subgenus *Omaladera*)

Material and methods

Taxon sampling and characters

Twenty two species belonging to *Stilbolemma* and four separate species' groups of *Maladera* (subgenus *Macroserica*, *Maladera*, *Cephaloserica*, and *Omaladera*) were included in the cladistic analysis. *Stilbolemma sericea* was chosen as the outgroup taxon due to its close relationship to the ingroup taxa based on shared apomorphies of 'modern' Sericini (chapter 3.1), but being with high probability not part of the ingroup. Character description and coding was based on 25 species belonging to four genera (see appendix A 3.2.2). The choice of the taxa included into analysis was mainly based on present and historical classification of the species and genera of the genus *Maladera* (e.g. Reitter 1902, Medvedev 1952b). Forty-seven adult characters were scored for this analysis. The character states are illustrated in Figs 38-40.

Phylogenetic analysis

The 47 characters (34 binary and 13 multistate) were all unordered and equally weighted. Inapplicable characters were coded as "-", while unknown character states were coded as "?" (Strong and Lipscomb 1999). The parsimony analysis was performed in NONA 2.0 (Goloboff 1999) using the parsimony ratchet (Nixon 1999) implemented in NONA, run with WINCLADA vs. 1.00.08 (Nixon 2002) as a shell program. Two hundred iterations were performed (one tree hold per iteration). The number of characters to be sampled for reweighting during the parsimony ratchet was determined to be 4. All searches were done under the collapsing option "ambiguous" which collapses every node with a minimum length of 0. State transformations were considered to be apomorphies of a given node only if they were unambiguous (i.e., without arbitrary selection of accelerated or delayed optimization) and if they were shared by all dichotomised most parsimonious trees. Bremer support (Bremer 1988, 1994) and parsimony jackknife percentages (Farris et al. 1996) were evaluated using NONA. The search was set to a Bremer support level of 12 (based on the number of unambiguous character changes for each node given by WINCLADA), with seven runs (each holding a number of trees from 100 to 500 times multiple of suboptimal tree length augmentation) and a total hold of 8000 trees. The jackknife values were calculated using 100 replications and a 100 search steps (mult*N) having one starting tree per replication (random seed 0). Character changes were mapped on the consensus tree using WINCLADA.

A second analysis with PAUP 3.1.1. (Swofford 1993) running a heuristic search performing TBR branch-swapping (MULPARS option in effect) with branches having maximum length zero collapsed to polytomies. Successive weighting (Farris 1969) was used to further evaluate phylogenetic relationships. This method uses *post hoc* character weighting based on the fit of each character as applied to the trees currently in memory. Thus, the 'quality' of the character data is used rather than intuitive feeling regarding weighting of characters. Although this method increases the assumptions in the analysis (Siebert 1992), its is useful for analysing phylogenetic pattern when characters exhibit a high level of homoplasy. Characters were reweighted based on the rescaled consistency index (rc). The maximum value "best fit" option was used, the base weight was set at 100, and indices were truncated. Tree searches continued until the character weights no longer changed (Farris 1988) or until identical trees were found in consecutive searches (indicating stability in the trees).

Characters and character states

In describing character states, I refrain from formulating any hypothesis about their transformation. In particular, coding does not imply whether a state is derived or ancestral. The data matrix is presented in appendix B 3.2.2.

Head

1. *Labroclypeus*: (0) flat (Figs 38C,E,F); (1) moderately convex medially (Fig. 38D); (2) with strong transverse elevation medially (Figs 38A,B).
2. *Labroclypeus, punctation*: (0) simple (Figs 38A,C,E); (1) rugose (Figs 38B,D).
3. *Labroclypeus, anterior angles*: (0) rounded (Figs 38A,B,D,E); (1) bluntly angled (Figs 38C,F).
4. *Labroclypeus, anterior margin medially*: (0) distinctly sinuate (Figs 38A-E); (1) straight.
5. *Labroclypeus, lateral margin behind labrum*: (0) not incised (Figs 38A,B,D,E); (1) incised (Fig. 38C,F); (2) 0&1.
6. *Labroclypeus anterior angles*: (0) simple (Figs 38A,B,D,E); (1) strongly reflexed (Figs 38C,F).
7. *Lateral margin of the labroclypeus and margin of the ocular canthus produced into*: (0) a distinct angle (Figs 38A,D,E); (1) a very indistinct angle (Figs 38B,C).
8. *Frons*: (0) glabrous (Figs 38A-E); (1) with a transverse row of setae directed posteriorly.
9. *Frons*: (0) dull (Figs 38B,C,F); (1) shiny (Figs 38A,D,E).
10. *Eyes, size*: (0) median (ratio ocular diameter/ interocular width > 0.5) (Figs 38B-E); (1) small (ratio ocular diameter/ interocular width < 0.5) (Fig. 38A); (2) very large (ratio ocular diameter/ interocular width ~ 0.8).

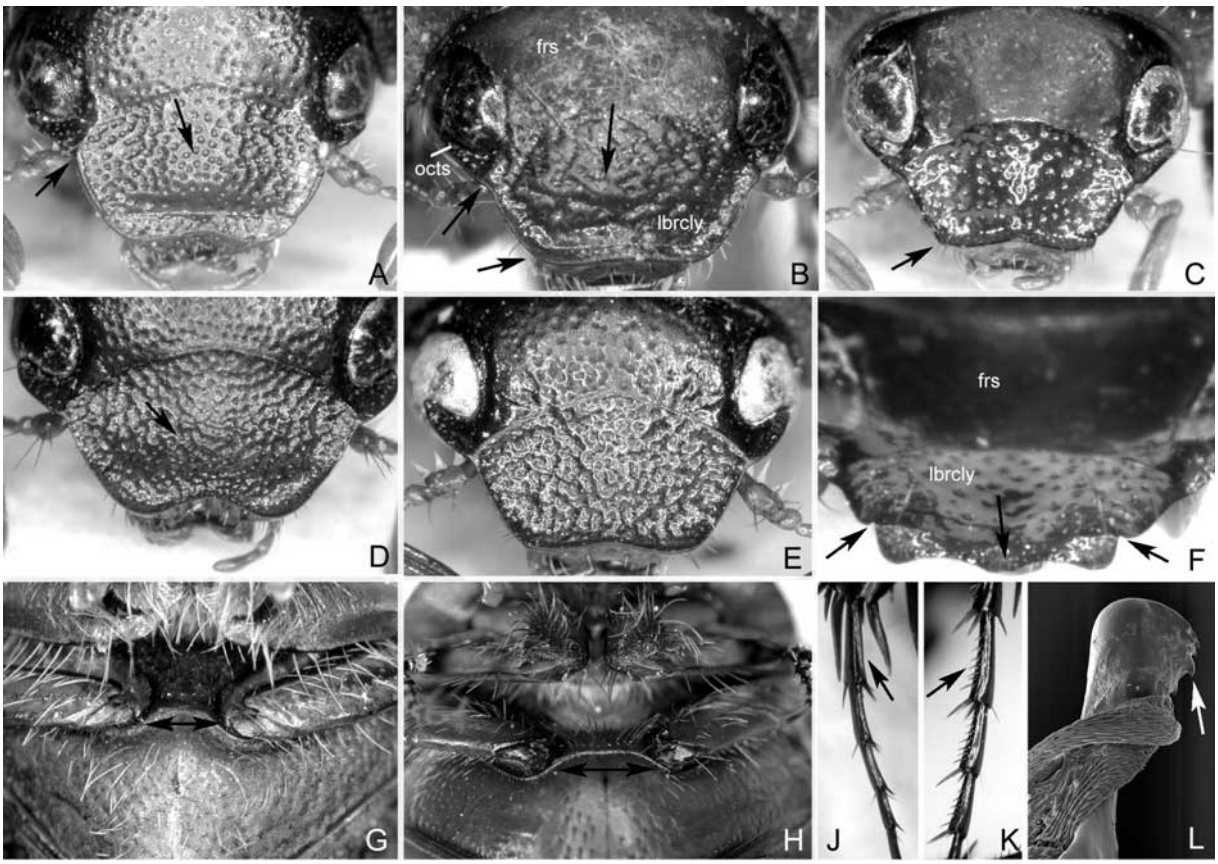

Fig. 38. A: *Stilbolemma sericea*; **B:** *Maladera himalayica*; **C, F:** *M. dierli*; **D:** *M. taurica*; **E, G, K:** *M. holosericea*; **H, J:** *M. insanabilis*; **L:** *M. simlana*, apex of right paramere. **A-E:** head, dorsal view; **F:** head, caudodorsal view; **G, H:** width of meso- and metasternum between the mesocoxae; **J, K:** metatarsomeres, ventral view (not to scale).

11. *Antenna, number of antennomeres*: (0) ten; (1) nine.

Thorax

12. *Body, dorsal surface*: (0) dull; (1) shiny.
13. *Body, coloration of dorsal surface*: (0) reddish brown; (1) blackish; (2) dark brown.
14. *Mesosternum between mesocoxae*: (0) narrow (narrower than mesofemur wide) (Fig. 38G); (1) wide (wider than mesofemur) (Fig. 38H).
15. *Elytra, apical border*: (0) glabrous; (1) with a rim of fine microtrichomes.

Legs

16. *Metafemur, posterior margin dorsally*: (0) not serrate; (1) serrate.
17. *Metafemur, between the two longitudinal hair rows*: (0) coarsely punctate; (1) smooth or very superficially punctate.
18. *Metafemur, distance between punctures of the anterior hair row:* (0) small; (1) large; (2) very small.
19. *Metatibia, basal external group of spines*: (0) at 1/3 or less of metatibial length (Fig. 39A); (1) at half metatibial length (Fig. 39B).
20. *Metatibia, interior spines on apical face*: (0) absent (Fig. 39G); (1) present (Fig. 39F).
21. *Metatibia, widest*: (0) at apex (Fig. 39B); (1) at middle (Fig. 39A).
22. *Metatibia, apex interiorly close to tarsal insertion*: (0) bluntly angled, not truncate (Fig. 39E); (1) bluntly angled, slightly concavely sinuate (Fig. 39C); (2) moderately truncate (Fig. 39D).
23. *Metatarsomere I in relation to superior spine of the metatibia*: (0) little longer or equal in length; (1) distinctly longer; (2) twice as long.
24. *Metatarsomere I-IV, pilosity*: (0) present (Fig. 38K); (1) absent (Fig. 38J).
25. *Tarsi, dorsal punctation*: (0) present; (1) absent.
26. *Metatarsomeres, subventral carina beside serrated ventral carina*: (0) distinct and robust (Fig. 38J); (1) indistinct, very weak (Fig. 38K).

Male genitalia

27. *Phallobase*: (0) symmetrical (Figs 39H,J); (1) asymmetrical (Figs 39K-R).
28. *Phallobase, distally*: (0) dorsoventrally flattened (Fig. 39S); (1) not dorsoventrally flattened (Figs 39T-X).
29. *Phallobase apically, between insertion of parameres*: (0) widely concavely sinuate (Fig. 39J,K); (1) produced medially (Figs 39L,N-R); (2) produced sublaterally-medially (Fig. 39M).
30. *Phallobase at right side apically*: (0) not produced (Figs 40C,E-G,K); (1) weakly but sharply produced ventrolaterally (Figs 40A,D); (2) strongly produced ventrolaterally (Fig. 40B).
31. *Phallobase preapically, dorsal portion*: (0) evenly depressed (Figs 39S,T,V, 40F-H,K,L,N); (1) abruptly depressed (Fig. 39W); (2) not depressed (Fig. 39U, 40A,B).
32. *Parameres*: (0) symmetrical (Figs 39H,J); (1) asymmetrical (Figs 39K-R).
33. *Ratio of right/ left paramere*: (0) subequal in length (1:1) (Figs 39J,K,P,S,T, 40E,F,J,M); (1) left paramere distinctly longer than the right until about half as long as the right (2:1) (Fig. 40N); (2) left paramere about four times shorter than the right (4:1) (Figs 39L,R,W,X); (3) left paramere strongly reduced, more than six times shorter than the right (6:1) (Figs 39M,U,V).
34. *Parameres*: (0) both simple (Figs 39J,L-R,T-X, 40A-E,H-N); (1) both with two or more distally directed lobes (Fig. 40F); (2) right paramere with two or more distally directed lobes (Fig. 40G).
35. *Right paramere, distal apodeme*: (0) not shortened (Figs 39J,K,M,Q-S,W,X, 40H,L,N); (1) shortened (Figs 39L,N-P,U,V).

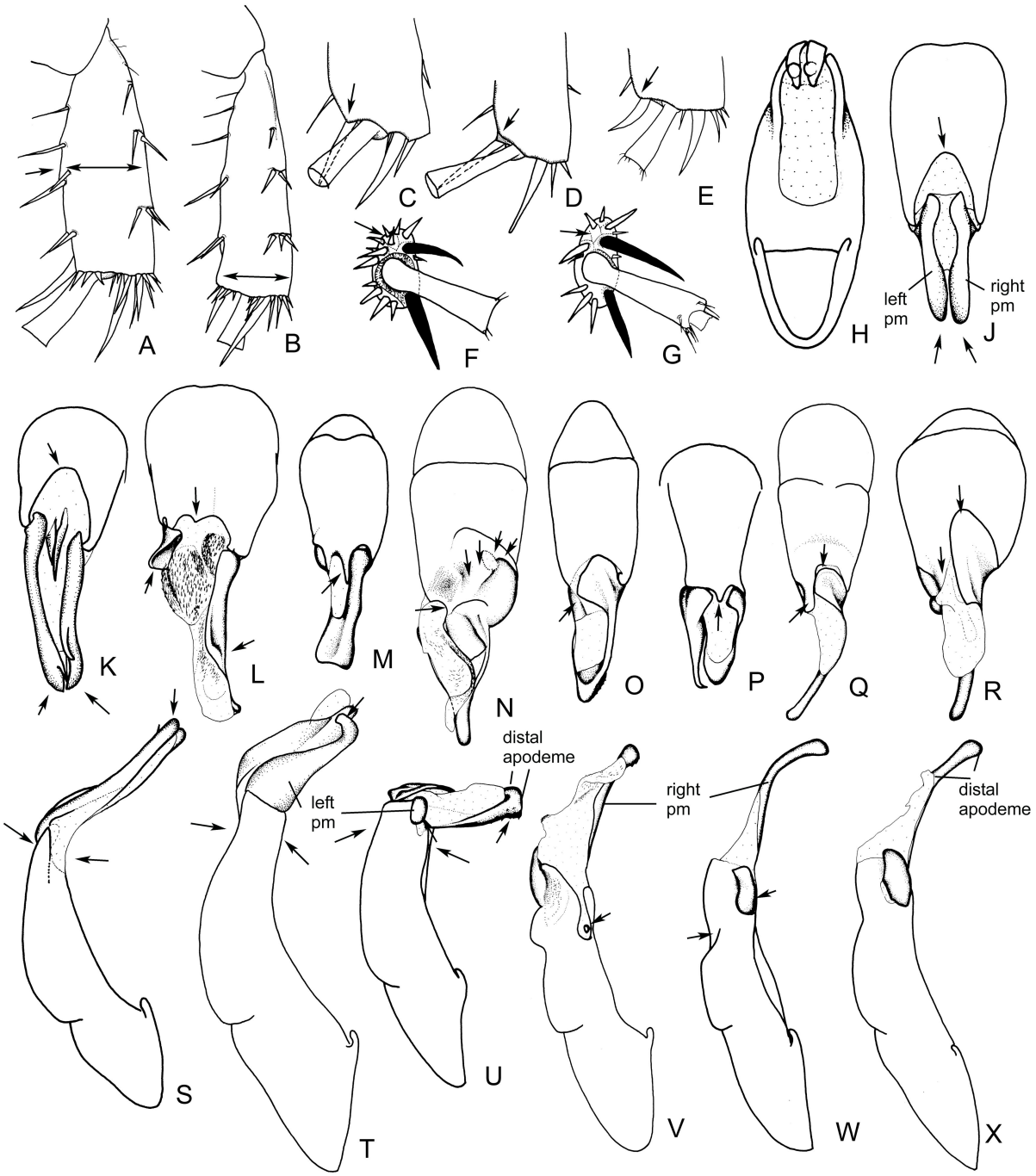

Fig. 39. A, C, T: *Maladera spectabilis*; **B, D, R:** *M. himalayica*; **E:** *M. insanabilis*; **F:** *M. renardi*; **G:** *Pleophylla* sp.; **H:** *Nipponoserica koltzei*; **J:** *Stilbolemma sericea*; **K, S:** *M. holosericea*; **L:** *M. stevensi*, **M:** *M. gardneri*; **N, V:** *M. simlana*; **O:** *M. dierli*; **P:** *M. cardoni*; **Q, W:** *M. thakkholae*; **U:** *M. sprecherae*, **X:** *M. immunda* **A, B:** metatibia, lateral view; **C-E:** apex metatibia, medial view; **F, G:** apex metatibia, caudal view; **H:** aedeagus, ventral view; **J-R:** parameres, dorsal view; **S-X:** aedeagus, left side lateral view (not to scale).

36. *Right paramere, distal apodeme*: (0) unarmed (Figs 39J-M,P-T,W,X, 40A-N); (1) armed with small teeth and spines (Figs 38L, 39U,V).
37. *Right paramere, basal lobe*: (0) absent (Figs 39J-M); (1) present (Figs 39N,O,Q,R).
38. *Right paramere, separate basal plate*: (0) absent (Figs 40A-D,F,G,K); (1) present (Fig. 40E).
39. *Right paramere*: (0) bent at middle ventrally (Figs 39W,X, 40B,C,H,K,L); (1) not bent ventrally, straight (Figs 39S,V, 40G,N).

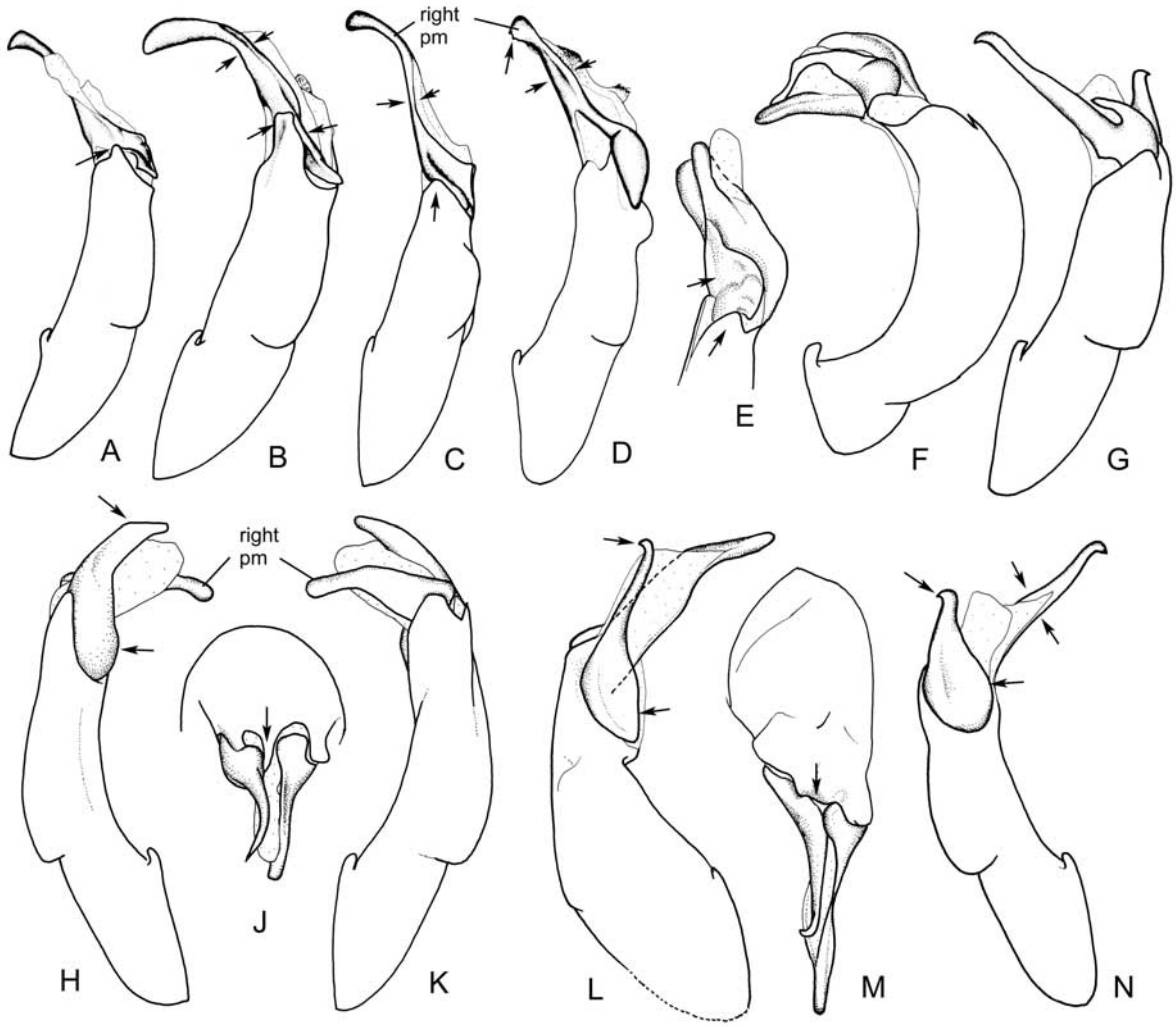

Fig. 40. A: *Maladera incola*; **B:** *M. joachimi*; **C:** *M. thakkholae*; **D:** *M. simlana*; **E:** *M. spectabilis*; **F:** *M. taurica*; **G, N:** *M. orientalis*; **H-K:** *M. cariniceps* (Lectotype); **L, M:** *M. lignicolor*. **A-D, F, G, K:** aedeagus, right side lateral view; **E:** parameres, right side lateral view; **H, L, N:** aedeagus, left side lateral view; **J, M:** parameres, dorsal view (not to scale).

40. *Right paramere*: (0) not dorsoventrally flattened basally (Figs 40A,D-N); (1) dorsoventrally flattened basally (Figs 40B,C).
41. *Basal lobe of right paramere*: (0) evenly widened basally (Figs 39Q,R); (1) abruptly widened basally and distally subequal in width (Fig. 39O); (2) fused medially with dorsal median process of the phallobase (Fig. 39N).
42. *Right paramere, mesally*: (0) narrowed, considerably narrower than apex of the phallobase (Figs 39J,K,Q); (1) widened, as wide as the apex of the phallobase (Figs 39M-O,R).
43. *Basal lobe of right paramere basally*: (0) short and semicircular (Figs 39O,Q); (1) prolonged (Fig. 39R).
44. *Left paramere*: (0) straight or bent ventrally at apex (Fig. 39S, 40H); (1) bent dorsally at apex (Figs 39T,W,X, 40L,N); (2) spherical (Fig. 39U,V).
45. *Left paramere apically*: (0) pointed; (1) rounded.
46. *Insertion of left paramere*: (0) at the same level as the right (Figs 39J,K,P); (1) displaced basally (Figs 39L-O,Q,R, 40J,L).
47. *Left paramere basally*: (0) not strongly widened (Figs 39S-X); (1) strongly widened and convexly elevated (Figs 40H,L,N).

Results

The analysis of 47 adult characters with the parsimony ratchet implemented in NONA with the above mentioned settings yielded 33 equally parsimonious trees of 113 steps (CI: 0.54 and RI: 0.75). Repeating the search ten times I obtained the same statistics as above. The characters 27 and 32 resulted uninformative in the present data set. The strict consensus of these trees, with jackknife values and Bremer support, is presented in Fig. 41. Repeating the parsimony ratchet with modified settings (1000 iterations and ten trees hold per iteration with ten sequential ratchet runs) did not result in a shorter tree or a modified topology of the strict consensus tree, but it did increase the number of equally parsimonious trees. The tree topology was not affected by altering ACCTRAN or DELTRAN optimization.

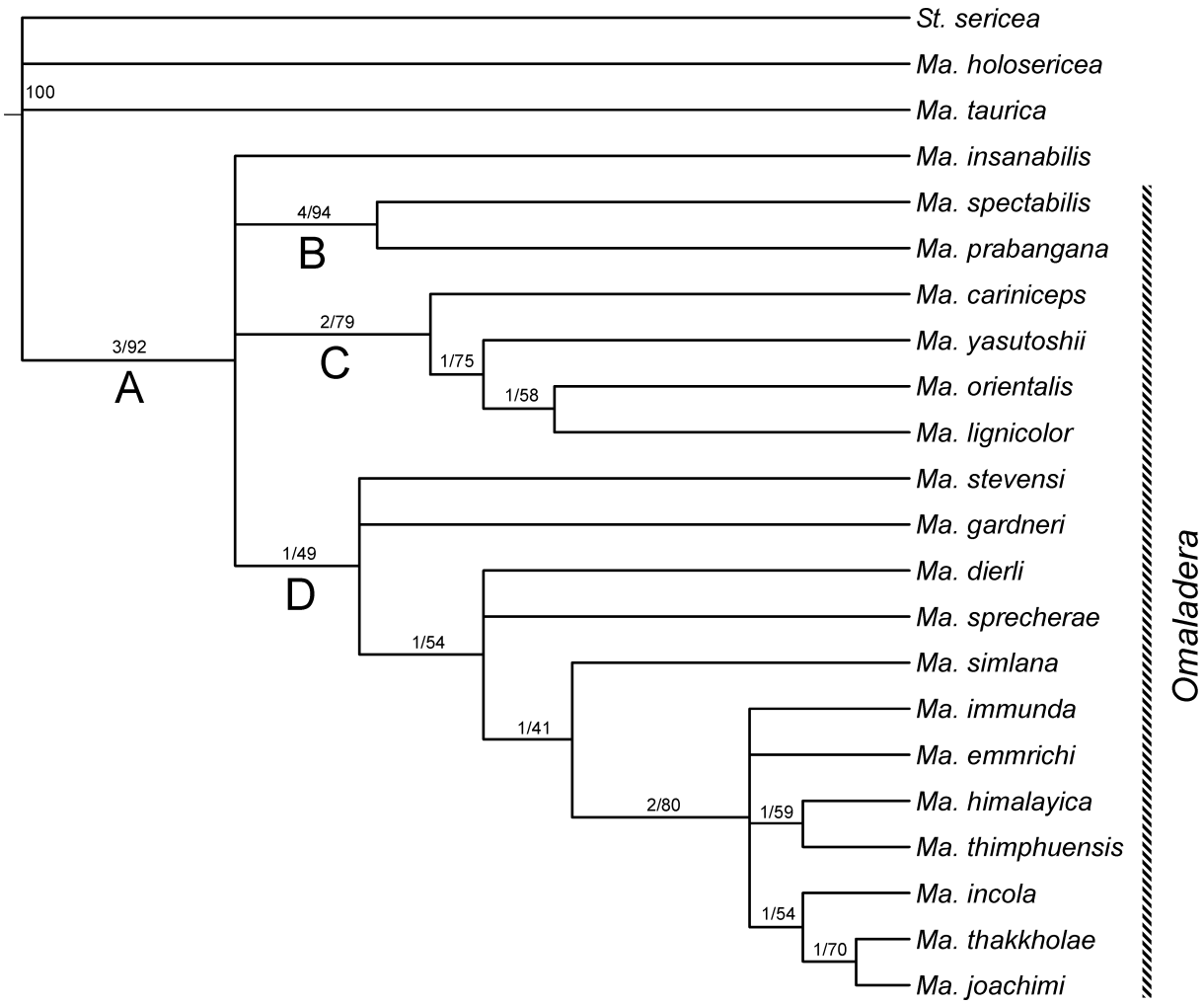

Fig. 41. Strict consensus of the 33 equally parsimonious trees with a length of 113 steps (CI: 0.54 and RI: 0.75); above each branch support indices (Bremer support/ jackknife values) (*Ma.*= *Maladera*, *St.*= *Stilbolemma*).

The strict consensus (Fig. 41) shows one major monophyletic clade (node A, Bremer support: 3, jackknife value: 92 %) within the ingroup which includes the representatives of the subgenus *Cephaloserica* (*M. insanabilis*) and the representatives of the subgenus *Omaladera*. However, from the consensus tree the monophyly of the subgenus *Omaladera* is not evident due to basal polytomy of the clade which divides subsequently into four lineages (Fig. 41), (1) *M. insanabilis*; (2) node B (*M. spectabilis* + *M. prabangana*); (3) node C (*M. cariniceps*, *M. yasutoshii*, *M. orientalis*, and *M. lignicolor*); and (4) node D containing all

Himalayan taxa of *Omaladera*, (*M. stevensi*, *M. gardneri*, (*M. dierli*, *M. sprecherae* (*M. simlana* (*M. immunda*, *M. emmrichi* (*M. himalayica*, *M. thimphuensis*), (*M. incola* (*M. thakkholae*, *M. joachimi*))))). Due to a limited number of characters available for the analysis and the high level of homoplasy, the branch support is generally low (see Fig. 41).

The heuristic search with PAUP 3.1.1. (Swofford 1999) yielded six equally parsimonious trees of 114 steps (CI: 0.54, RI: 0.76) showing a very similar topology to the trees obtained by the NONA parsimony ratchet. The strict consensus tree of the search with equally weighted characters is shown in Fig. 42A. It provides identical principal monophyletic clades (e.g. *Cephaloserica* + *Omaladera* and monophyletic lineages of the nodes B, C, D). To assume the information of the equally parsimonious trees resulted from the parsimony ratchet with equally weighted characters, a majority rule consensus tree was generated (Fig. 43).

To further examine phylogenetic pattern, the unweighted characters were reanalysed after successive character weighting (Farris 1969) based on the rescaled consistency (rc) index yielding four equally parsimonious trees. The strict consensus tree from the most parsimonious trees based on successive character weighting shows compared to the strict consensus of the original data set a slightly modified topology. It provides in parts a higher resolution, only (Fig. 42B).

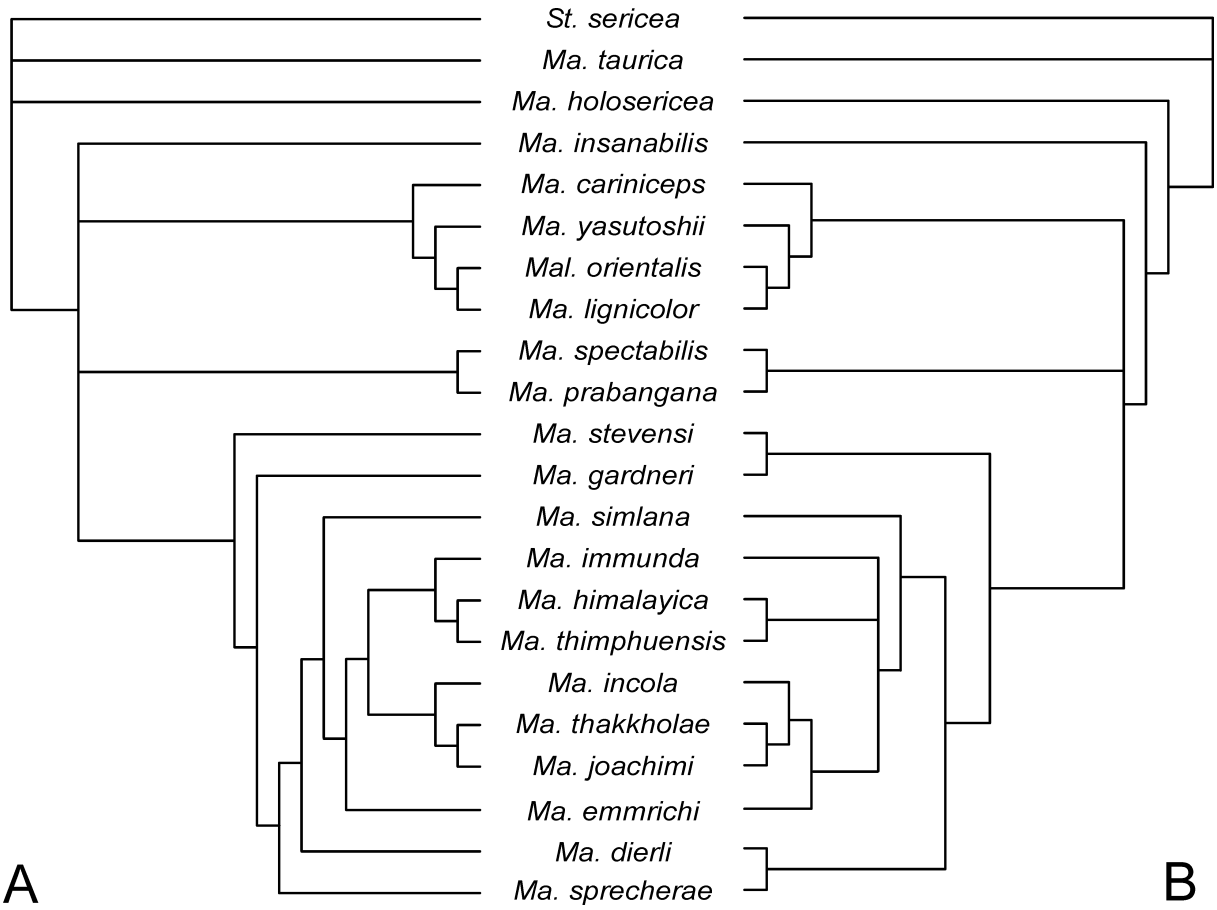

Fig. 42. (A) Strict consensus tree (of six equally parsimonious trees, 114 steps, CI: 0.544, RI: 0.765) resulting from heuristic search with PAUP 3.1.1. with unweighted characters, and **(B)** the strict consensus tree (of four equally parsimonious trees) resulting from heuristic search with PAUP after successive weighting by the rescaled consistency index (*Ma.*= *Maladera*, *St.*= *Stilbolemma*).

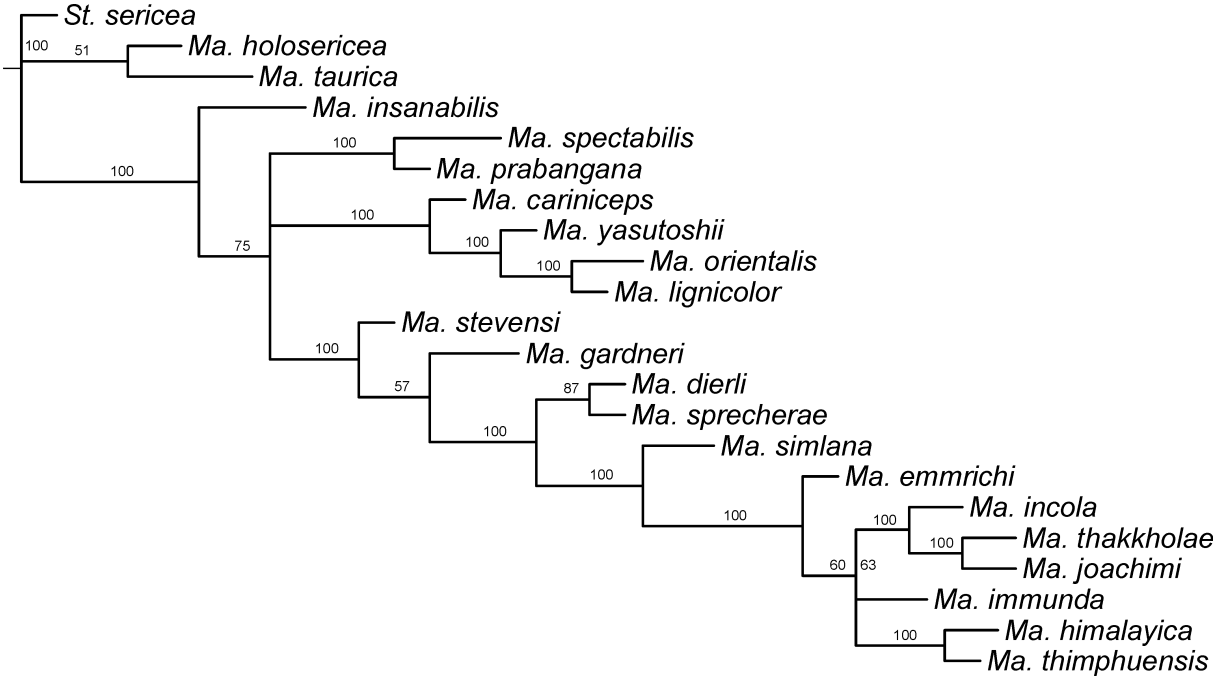

Fig. 43. Majority rule consensus tree of the 33 most parsimonious trees yielded by parsimony ratchet (NONA analysis) (113 steps, CI: 0.54 and RI: 0.75), above each branch is given the frequency (%) of a node among all MPTs, (*Ma.*= *Maladera*, *St.*= *Stilbolemma*).

Discussion

Both, the majority rule consensus tree from MPTs of the parsimony ratchet and the strict consensus which resulted from heuristic search with PAUP based on successive weighting were well resolved for: (1) the basal relationships, in particular providing evidence for the monophyly of the subgenus *Omaladera*, and (2) relationships of the Himalayan taxa of *Omaladera*.

From the thirty three equally parsimonious trees generated with the parsimony ratchet (113 steps) which yielded in contrast to the heuristic search (114 steps) with PAUP the shortest tree, one preferred phylogenetic tree was chosen to illustrate the character evolution of *Omaladera* (Fig. 44). This tree corroborates the majority rule consensus tree derived from parsimony ratchet and the strict consensus that resulted from heuristic search based on successive weighting with PAUP.

The tree topology of the majority rule consensus tree (Fig. 43) as well as the strict consensus tree obtained after heuristic search with reweighted characters (Fig. 42B) provide evidence for the hypothesis that the subgenus *Omaladera* is a monophyletic group. This subgenus was once established by Reitter (1896) for two species (*M. diffinis* (Reitter, 1896), *M. cavifrons* (Reitter, 1896)), presently, both are regarded to be synonymous with *M. orientalis* (Motschulsky, 1857). To facilitate the classification and identification of the *Maladera* species, additional taxa were later included into the subgenus (Ahrens 2004b). In the framework of this study, the monophyly of *Omaladera* is supported by the following apomorphies (Fig. 44): (1) lateral margins of labroclypeus and of ocular canthus produce a very indistinct angle (Figs 38B,C; 7:1); (2) basal external group of metatibial spines at half metatibial length (Figs 39B, 19:1). Its sister relationship with the subgenus *Cephaloserica* is based on a number of unambiguous apomorphies not concerned by homoplasy: (1) frons dull (9:0); (2) mesosternum between mesocoxae wider than the mesofemur (14:1); (3) phallobase between the insertion of the parameres produced mesoapically (29:1).

Maladera spectabilis and *M. prabangana* constitute a well supported clade (node B, Bremer support: 4, jackknife value 94 %). Both they are the representatives of a lineage which includes additional taxa occurring as far as known only in Indochina and southern

China. These taxa share the following unambiguous and non-homoplasious apomorphies: (1) anterior margin of labroclypeus medially straight (4:1); (2) distance between punctures of anterior hair row of metafemur large (18:1); (3) right paramere, with separate basal plate (38:1, Fig. 44). Furthermore, they are characterized (unambiguous apomorphies but concerned by homoplasy) by small eyes (10:1) and by a glabrous apical border of elytra (15:0).

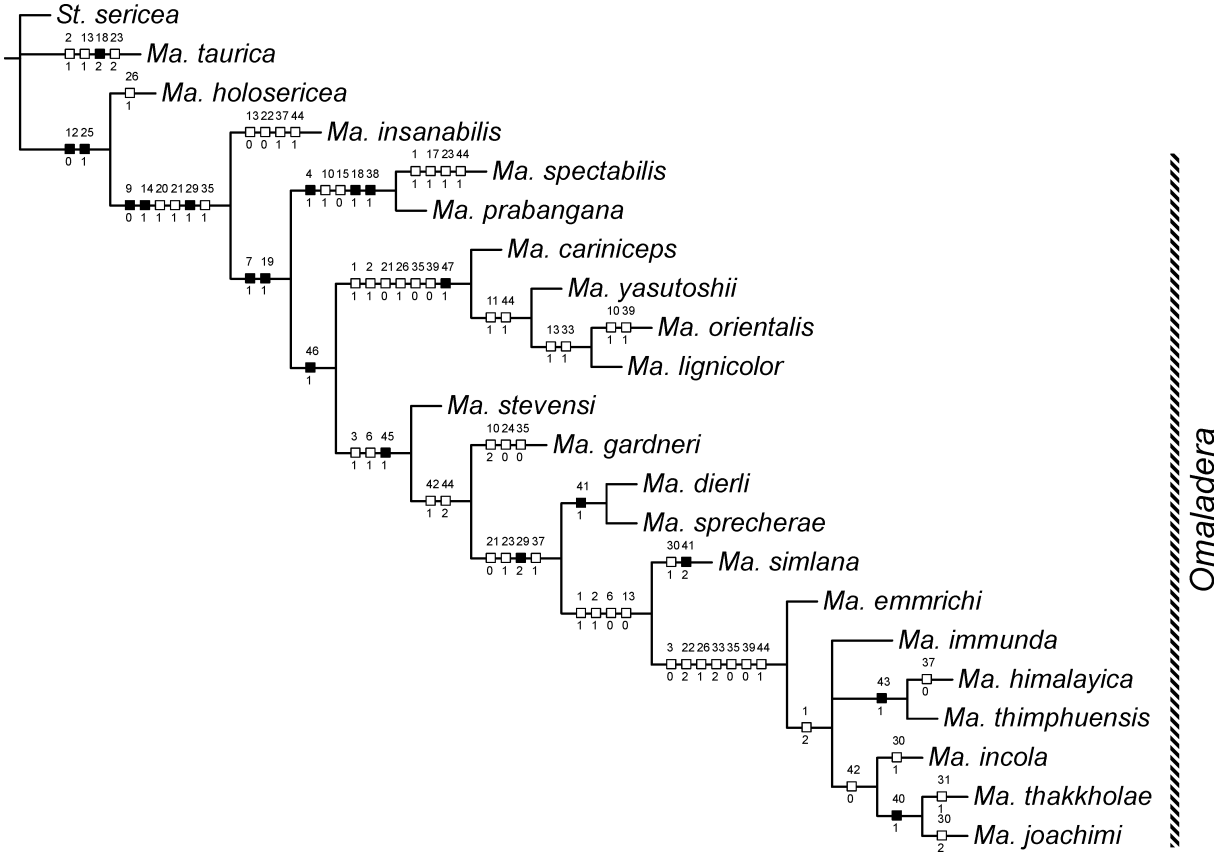

Fig. 44. Preferred tree of the 33 equally parsimonious trees with a length of 113 steps (CI: 0.54 and RI: 0.75) showing character changes and apomorphies mapped by state (discontinuous characters are mapped as homoplasy and only unambiguous changes are shown, unsupported nodes collapsed and using proportional branch lengths). The tree was chosen in reference to the majority rule consensus of the WINCLADA analysis and the strict consensus tree of the PAUP analysis based on successive reweighting (full squares: non-homoplasious character states; empty squares: homoplasious character states) (*Ma.*= *Maladera*, *St.*= *Stilbolemma*).

A second well supported clade is the lineage of node C (Bremer support: 2, jackknife value 79 %). These species share the basally strongly widened and convexly swollen left paramere (47:1, Figs 3H,L,N) being the only character not concerned by homoplasy. Furthermore, the following apomorphies support this node: (1) labroclypeus moderately convex medially (1:1); (2) labroclypeus with rugose punctation (2:1); (3) metatibia widest at apex (21:0); (4) distal apodeme of right paramere not shortened (35:0); and (5) right paramere bent at middle ventrally (39:0). This clade has a geographical range limited to the north-eastern Palearctic Asia (Fig. 46) embracing all major archipelagos (Taiwan, Japan, Ryuku Islands) (Nomura 1973). In addition to *M. cariniceps*, *M. yasutoshii*, *M. orientalis*, and *M. lignicolor*, I hypothesize that *M. oshimana okinawana* Nomura, 1964, *M. oshimana oshimana* Nomura, 1962, and *M. oshimana sakishimana* Nomura, 1964, which all have been described from the Ryuku Islands, should be assigned to this lineage based on the characters given in their original descriptions and illustrations of male genitalia. The majority of the species in this clade possess strong infraspecific variation making it more difficult to distinguish between geographic forms (local populations or subspecies) and simple variability. Thus, a more

detailed examination of the diversification of this lineage is reserved for future studies after detailed revision of the morphological variation in the group.

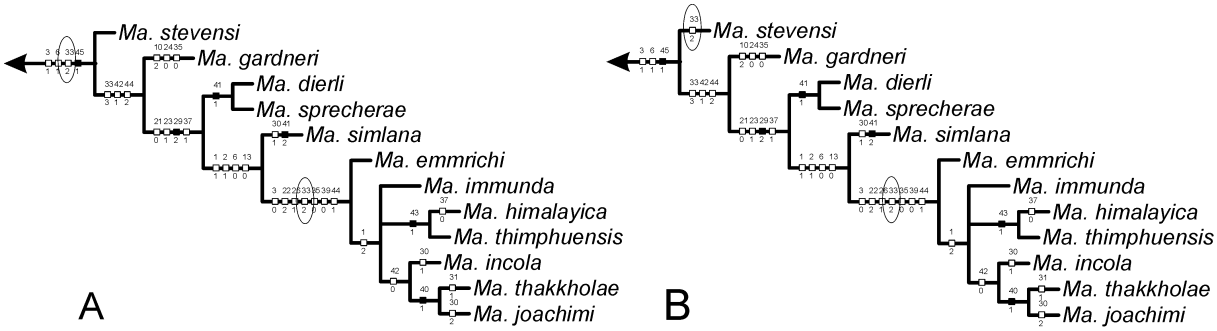

Fig. 45. Character conflict between ACCTRAN and DELTRAN optimization in the preferred tree of the 33 equally parsimonious trees (113 steps, CI: 0.54 and RI: 0.75) showing apomorphies mapped by state (discontinuous characters are mapped as homoplasy, unsupported nodes collapsed and using proportional branch lengths) (full squares: non-homoplasious character states; empty squares: homoplasious character states) (*Ma.*= *Maladera*).

Hypothesized monophyly of the Himalayan *Omaladera* species' clade results from all four approaches of tree search involved for this study and it is based on the following unambiguous apomorphies: (1) anterior angles of labroclypeus bluntly angled (3:1); (2) anterior angles of labroclypeus strongly reflexed (6:1); and (3) left paramere apically rounded (45:1). Additionally, in the preferred most parsimonious tree (Fig. 7) monophyly is supported by another apomorphy under ACCTRAN optimization criterion (Fig. 45A): (4) left paramere about four times shorter than the right (33:2). The reduction of the length of the left paramere in the Himalayan *Omaladera* species is unique for the Sericini. Based on the scheme of character evolution in Fig. 45A, which was resulting from hypothesized phylogeny, the left paramere is shortened even more (33:3) when the left paramere is more than six times shorter than the right. This step, however, is subject to a subsequent reversal (under ACCTRAN optimization, right circle, Fig. 45A), while under DELTRAN optimization the strongly shortened left paramere (33:2) results to have developed twice (circles, Fig. 45B), in *M. stevensi* and in the clade (*M. emmrichi* (*M. immunda*, (*M. himalayica*, *M. thimphuensis*), (*M. incola* (*M. thakkholae*, *M. joachimi*)))).

Implications on taxonomy, evolution, and biogeography

Although the current stage of exploration of Asian sericine fauna is still incomplete (with exception of the Nepal Himalaya), the record and the taxonomic knowledge on Asian sericine fauna (Ahrens, unpublished results) have improved in the last decade notably. These investigations provide evidence, that the cumulative geographical ranges of the taxa of the three lineages (Fig. 46) of *Omaladera* do not overlap significantly. Within the three regions depicted in Fig. 46 each lineage diversified independently, and the present phylogenetic hypothesis (Figs 41-44) is not consistent with a faunal exchange in history concerning the extant representatives or taxa of the stem lineage of each of the three clades.

To understand the main far-reaching factors for the Himalayan diversification, the altitudinal distribution of the species has to be considered. All species occur within a range from 300 to 3300 meters (Fig. 47), namely from the hilly to the upper montane zone. However, the interval from 1100 to 2800 meters is preferred habit as evident from frequency of record along the altitudinal gradient (Fig. 47). The species are absent in the lowland below 300 meters, thus explaining a barrier for direct dispersal from the Himalaya to the climatically similar Khasi Hills in Meghalaya (India) through the lowland. Based on this altitudinal

distribution pattern, taxa of the clade would become permanently separated by mountain ranges higher than 4000 meters once gained this altitudinal distribution pattern. Such a geographical limit we encounter presently for example in the Great Himalayan range, in the Tibetan Plateau, as well as in its eastern chains from Gansu (China) in the north to Yunnan (China)/ northern Burma (Myanmar) in the south. Onset of orogeny in these regions is hypothesized to be in late Eocene (Tapponnier et al. 2001). Reaching enough height, these ranges must have become geographical barriers for dispersal. Such an high elevation could have been achieved already during early Miocene, since fossil leaf assemblages provide evidence that the altitude in parts of the southern Tibetan Plateau probably has remained unchanged for the past 15 Ma (Spicer et al. 2003). This could be considered as a minimum age for the Himalayan lineage (node D, Fig. 41), whose splitting (Fig. 44) from the northern Asian lineage (including *M. orientalis* etc.) (node C, Fig. 41) is consistent with such a separation event.

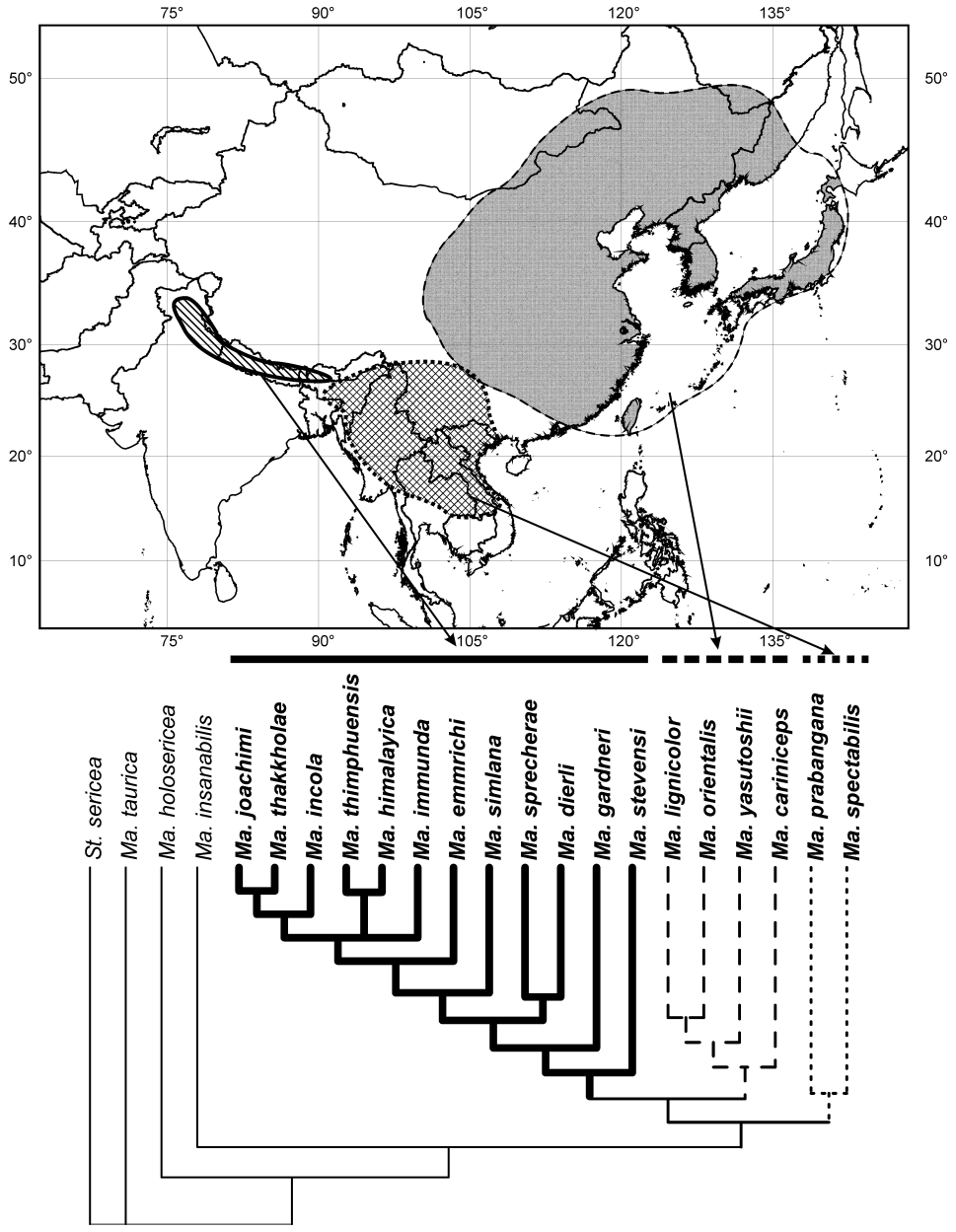

Fig. 46. The hypothesized phylogeny of the subgenus *Omaladera* (based on preferred most parsimonious tree, Fig. 7) placed into geographical context, showing that the three main clades are geographically separated and being divided into a Himalayan, an Indochinese, and a North-Asian one (*Ma.*= *Maladera*, *St.*= *Stilbolemma*).

High relief energy and strong climatic contrast (Dobremez 1976) presumably induced separation processes in periods of fluctuating climate, which must have affected the fauna and flora of southern Himalayan slope with a hilly-montane distribution, such as the taxa of *Omaladera*. Nevertheless, the size of distributional ranges of taxa in the Himalayan *Omaladera* lineage vary greatly: the two basal branching taxa, *M. stevensi* and *M. gardneri*, have a very restricted occurrence, while the taxa of the more apical lineages have more extensive ranges in the entire central and western Himalaya (e.g. *M. simlana*, *M. dierli*, and *M. emmrichi*). Taxa with more distal position in the tree are geographically limited within a small number of mountain massifs separated by deeply incised river valleys or valleys that are separated by high mountains.

Some of the distal *Omaladera* species are strictly parapatric wherefore they have been established originally as subspecies (Ahrens 2004b). However, phylogenetic analyses support the hypothesis, that *M. himalayica*, *M. incola*, *M. immunda*, and *M. thakkholae* are valid species. Corroborative evidence includes the range overlap and syntopic occurrence of the two distal sister taxa, *M. joachimi* and *M. thakkholae* (Fig. 48), indicating that also all taxa of their basal lineages (*M. immunda*, *M. incola,* and the last common ancestor of *M. himalayica* + *M. thimphuensis*) must be separate species. Conversely, present data set and tree topology provide no base to discuss the status (species or subspecies) of *M. himalayica* and *M. thimphuensis*. Additional phylogenetic research based on molecular data and molecular dating and further specimens for morphological examination from the geographical area between the two presently known ranges of the two taxa may be necessary to understand the speciation of *M. himalayica* and *M. thimphuensis.*

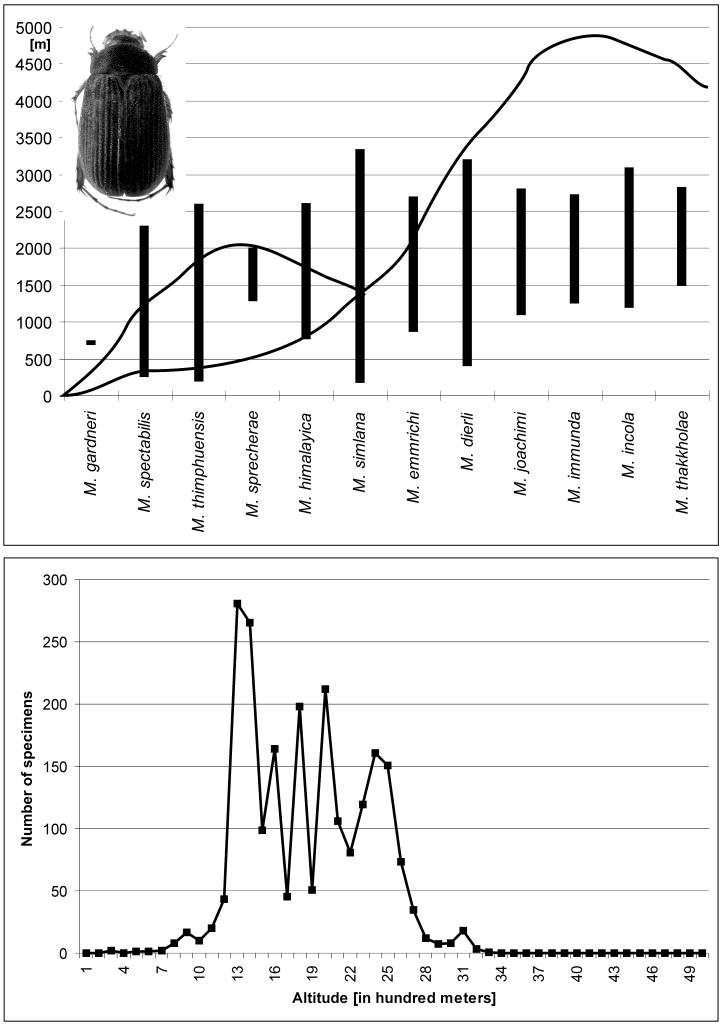

Fig. 47. Altitudinal distribution of the Himalayan taxa of the subgenus *Omaladera* showing (a) the entire interval of record data (above, (*M.*= *Maladera*) and (b) the total abundance in relation to altitude (in hundred metre steps) cumulated from all Himalayan *Omaladera* representatives (below) (*M. stevensi* was not

Faunistic exploration in the Himalaya is far from being completed and conclusions regarding the "endemic" basal lineages (*M. stevensi*, *M. gardneri*) should be considered only in relation to historical distributions. These hypothesized extensive Himalayan-wide distribution of stem lineage representatives of the Himalayan *Omaladera* and its basal taxa would be consistent with a evolutive scenario for *Omaladera* explaining the separate development of the tree principal lineages by geographical separation (Fig. 46).

Based on the hypothesized phylogeny of the apical lineages within the Himalayan *Omaladera* clade (Fig. 48), there is support that parapatric speciation played a dominant role during the process of diversification. In contrast to other Himalayan Sericini, the degree of endemism in *Omaladera* is relatively low. This may correspond with the wide ecological tolerances of most of their species.

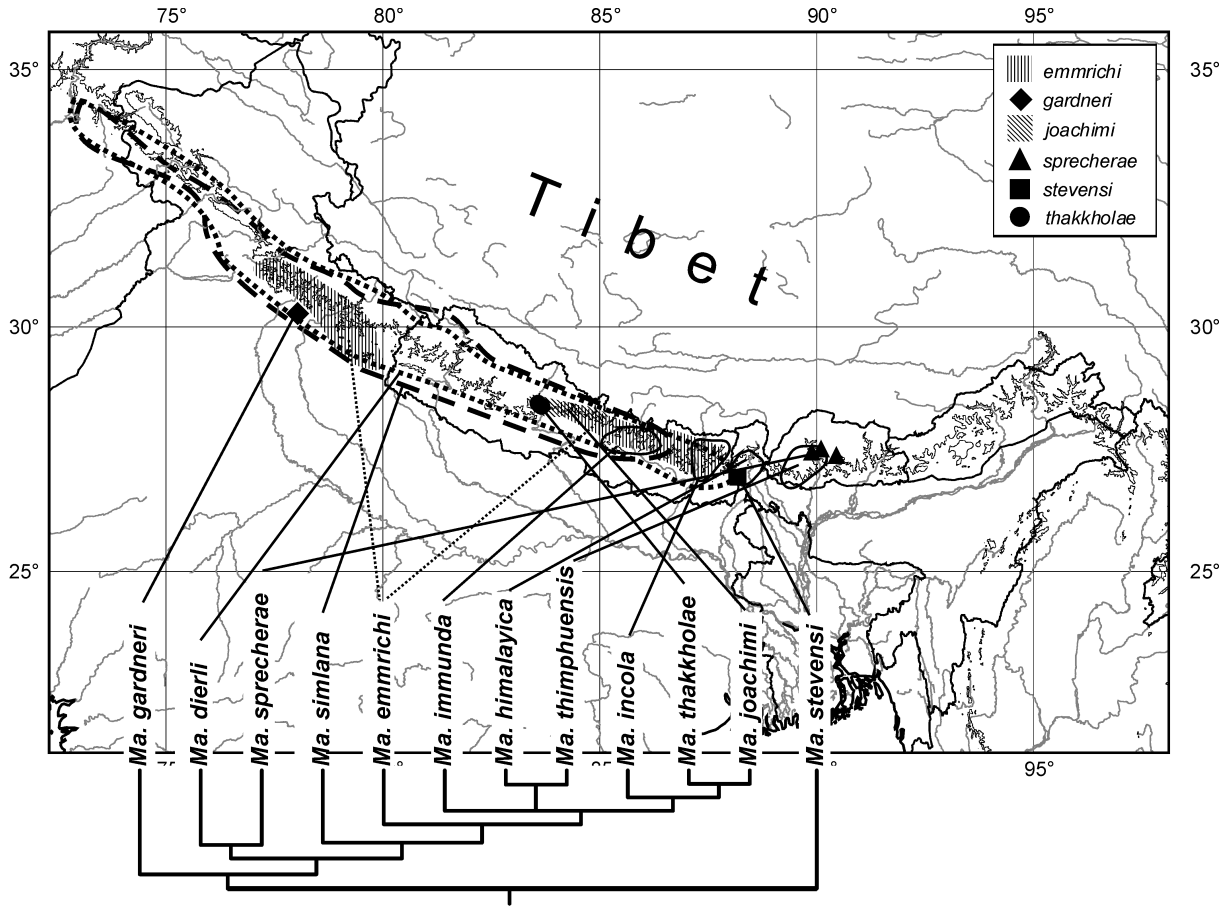

Fig. 48. The phylogenetic tree of the Himalayan taxa of the subgenus *Omaladera* with their respective distribution ranges (*Ma.*= *Maladera*).

Diversification of Himalayan *Omaladera* shows that the Himalaya is not only a region working as faunal bridge (Kurup 1990) being rather 'recently' invaded and occupied by an 'immigrated fauna' (Martens 1993). Based on phylogeny of *Omaladera*, it must be supposed that parts of its fauna (with reference to altitudinal gradient) have had a rather independent history for a rather long period. In fact, such a hypothesis would be consistent with some of the chorological classification concepts of comparative biogeographers (e.g. summarized in Mani 1974, de Latin 1967, Dobremez 1976, Martens 1993) establishing an own 'Himalayan' subcenter or respectively subregion. When explaining and conserving the rich biodiversity in the Himalaya, responsibility must assigned not only to the fact, that the region lies between Palearctic and Oriental realm building a borderline with a high vertical and horizontal faunal interchange, but, moreover, it provides an autochthonous heritage of great importance.